

Observation of $B_s^0 \rightarrow K^+ K^-$ and Measurements of Branching Fractions of Charmless Two-body Decays of B^0 and B_s^0 Mesons in $\bar{p}p$ Collisions at $\sqrt{s} = 1.96$ TeV

A. Abulencia,²³ D. Acosta,¹⁷ J. Adelman,¹³ T. Affolder,¹⁰ T. Akimoto,⁵⁵ M.G. Albrow,¹⁶ D. Ambrose,¹⁶ S. Amerio,⁴³ D. Amidei,³⁴ A. Anastassov,⁵² K. Anikeev,¹⁶ A. Annovi,¹⁸ J. Antos,¹ M. Aoki,⁵⁵ G. Apollinari,¹⁶ J.-F. Arguin,³³ T. Arisawa,⁵⁷ A. Artikov,¹⁴ W. Ashmanskas,¹⁶ A. Attal,⁸ F. Azfar,⁴² P. Azzi-Bacchetta,⁴³ P. Azzurri,⁴⁶ N. Bacchetta,⁴³ H. Bachacou,²⁸ W. Badgett,¹⁶ A. Barbaro-Galtieri,²⁸ V.E. Barnes,⁴⁸ B.A. Barnett,²⁴ S. Baroiant,⁷ V. Bartsch,³⁰ G. Bauer,³² F. Bedeschi,⁴⁶ S. Behari,²⁴ S. Belforte,⁵⁴ G. Bellettini,⁴⁶ J. Bellinger,⁵⁹ A. Belloni,³² E. Ben Haim,⁴⁴ D. Benjamin,¹⁵ A. Beretvas,¹⁶ J. Beringer,²⁸ T. Berry,²⁹ A. Bhatti,⁵⁰ M. Binkley,¹⁶ D. Bisello,⁴³ R. E. Blair,² C. Blocker,⁶ B. Blumenfeld,²⁴ A. Bocci,¹⁵ A. Bodek,⁴⁹ V. Boisvert,⁴⁹ G. Bolla,⁴⁸ A. Bolshov,³² D. Bortoletto,⁴⁸ J. Boudreau,⁴⁷ A. Boveia,¹⁰ B. Brau,¹⁰ C. Bromberg,³⁵ E. Brubaker,¹³ J. Budagov,¹⁴ H.S. Budd,⁴⁹ S. Budd,²³ K. Burkett,¹⁶ G. Busetto,⁴³ P. Bussey,²⁰ K. L. Byrum,² S. Cabrera,¹⁵ M. Campanelli,¹⁹ M. Campbell,³⁴ F. Canelli,⁸ A. Canepa,⁴⁸ D. Carlsmith,⁵⁹ R. Carosi,⁴⁶ S. Carron,¹⁵ M. Casarsa,⁵⁴ A. Castro,⁵ P. Catastini,⁴⁶ D. Cauz,⁵⁴ M. Cavalli-Sforza,³ A. Cerri,²⁸ L. Cerrito,⁴² S.H. Chang,²⁷ J. Chapman,³⁴ Y.C. Chen,¹ M. Chertok,⁷ G. Chiarelli,⁴⁶ G. Chlachidze,¹⁴ F. Chlebana,¹⁶ I. Cho,²⁷ K. Cho,²⁷ D. Chokheli,¹⁴ J.P. Chou,²¹ P.H. Chu,²³ S.H. Chuang,⁵⁹ K. Chung,¹² W.H. Chung,⁵⁹ Y.S. Chung,⁴⁹ M. Ciljak,⁴⁶ C.I. Ciobanu,²³ M.A. Ciocci,⁴⁶ A. Clark,¹⁹ D. Clark,⁶ M. Coca,¹⁵ G. Compostella,⁴³ M.E. Convery,⁵⁰ J. Conway,⁷ B. Cooper,³⁰ K. Copic,³⁴ M. Cordelli,¹⁸ G. Cortiana,⁴³ F. Crescioli,⁴⁶ A. Cruz,¹⁷ C. Cuenca Almenar,⁷ J. Cuevas,¹¹ R. Culbertson,¹⁶ D. Cyr,⁵⁹ S. DaRonco,⁴³ S. D'Auria,²⁰ M. D'Onofrio,³ D. Dagenhart,⁶ P. de Barbaro,⁴⁹ S. De Cecco,⁵¹ A. Deisher,²⁸ G. De Lentdecker,⁴⁹ M. Dell'Orso,⁴⁶ F. Delli Paoli,⁴³ S. Demers,⁴⁹ L. Demortier,⁵⁰ J. Deng,¹⁵ M. Deninno,⁵ D. De Pedis,⁵¹ P.F. Derwent,¹⁶ C. Dionisi,⁵¹ J.R. Dittmann,⁴ P. DiTuro,⁵² C. Dörr,²⁵ S. Donati,⁴⁶ M. Donega,¹⁹ P. Dong,⁸ J. Donini,⁴³ T. Dorigo,⁴³ S. Dube,⁵² K. Ebina,⁵⁷ J. Efron,³⁹ J. Ehlers,¹⁹ R. Erbacher,⁷ D. Errede,²³ S. Errede,²³ R. Eusebi,¹⁶ H.C. Fang,²⁸ S. Farrington,²⁹ I. Fedorko,⁴⁶ W.T. Fedorko,¹³ R.G. Feild,⁶⁰ M. Feindt,²⁵ J.P. Fernandez,³¹ R. Field,¹⁷ G. Flanagan,⁴⁸ L.R. Flores-Castillo,⁴⁷ A. Foland,²¹ S. Forrester,⁷ G.W. Foster,¹⁶ M. Franklin,²¹ J.C. Freeman,²⁸ I. Furic,¹³ M. Gallinaro,⁵⁰ J. Galyardt,¹² J.E. Garcia,⁴⁶ M. Garcia Sciveres,²⁸ A.F. Garfinkel,⁴⁸ C. Gay,⁶⁰ H. Gerberich,²³ D. Gerdes,³⁴ S. Giagu,⁵¹ P. Giannetti,⁴⁶ A. Gibson,²⁸ K. Gibson,¹² C. Ginsburg,¹⁶ N. Giokaris,¹⁴ K. Giolo,⁴⁸ M. Giordani,⁵⁴ P. Giromini,¹⁸ M. Giunta,⁴⁶ G. Giurgiu,¹² V. Glagolev,¹⁴ D. Glenzinski,¹⁶ M. Gold,³⁷ N. Goldschmidt,³⁴ J. Goldstein,⁴² G. Gomez,¹¹ G. Gomez-Ceballos,¹¹ M. Goncharov,⁵³ O. González,³¹ I. Gorelov,³⁷ A.T. Goshaw,¹⁵ Y. Gotra,⁴⁷ K. Goulianos,⁵⁰ A. Gresele,⁴³ M. Griffiths,²⁹ S. Grinstein,²¹ C. Grosso-Pilcher,¹³ R.C. Group,¹⁷ U. Grundler,²³ J. Guimaraes da Costa,²¹ Z. Gunay-Unalan,³⁵ C. Haber,²⁸ S.R. Hahn,¹⁶ K. Hahn,⁴⁵ E. Halkiadakis,⁵² A. Hamilton,³³ B.-Y. Han,⁴⁹ J.Y. Han,⁴⁹ R. Handler,⁵⁹ F. Happacher,¹⁸ K. Hara,⁵⁵ M. Hare,⁵⁶ S. Harper,⁴² R.F. Harr,⁵⁸ R.M. Harris,¹⁶ K. Hatakeyama,⁵⁰ J. Hauser,⁸ C. Hays,¹⁵ A. Heijboer,⁴⁵ B. Heinemann,²⁹ J. Heinrich,⁴⁵ M. Herndon,⁵⁹ D. Hidas,¹⁵ C.S. Hill,¹⁰ D. Hirschbuehl,²⁵ A. Hocker,¹⁶ A. Holloway,²¹ S. Hou,¹ M. Houlden,²⁹ S.-C. Hsu,⁹ B.T. Huffman,⁴² R.E. Hughes,³⁹ J. Huston,³⁵ J. Incandela,¹⁰ G. Introzzi,⁴⁶ M. Iori,⁵¹ Y. Ishizawa,⁵⁵ A. Ivanov,⁷ B. Iyutin,³² E. James,¹⁶ D. Jang,⁵² B. Jayatilaka,³⁴ D. Jeans,⁵¹ H. Jensen,¹⁶ E.J. Jeon,²⁷ S. Jindariani,¹⁷ M. Jones,⁴⁸ K.K. Joo,²⁷ S.Y. Jun,¹² T.R. Junk,²³ T. Kamon,⁵³ J. Kang,³⁴ P.E. Karchin,⁵⁸ Y. Kato,⁴¹ Y. Kemp,²⁵ R. Kephart,¹⁶ U. Kerzel,²⁵ V. Khotilovich,⁵³ B. Kilminster,³⁹ D.H. Kim,²⁷ H.S. Kim,²⁷ J.E. Kim,²⁷ M.J. Kim,¹² S.B. Kim,²⁷ S.H. Kim,⁵⁵ Y.K. Kim,¹³ L. Kirsch,⁶ S. Klimenko,¹⁷ M. Klute,³² B. Knuteson,³² B.R. Ko,¹⁵ H. Kobayashi,⁵⁵ K. Kondo,⁵⁷ D.J. Kong,²⁷ J. Konigsberg,¹⁷ A. Korytov,¹⁷ A.V. Kotwal,¹⁵ A. Kovalev,⁴⁵ A. Kraan,⁴⁵ J. Kraus,²³ I. Kravchenko,³² M. Kreps,²⁵ J. Kroll,⁴⁵ N. Krumnack,⁴ M. Kruse,¹⁵ V. Krutelyov,⁵³ S. E. Kuhlmann,² Y. Kusakabe,⁵⁷ S. Kwang,¹³ A.T. Laasanen,⁴⁸ S. Lai,³³ S. Lami,⁴⁶ S. Lammel,¹⁶ M. Lancaster,³⁰ R.L. Lander,⁷ K. Lannon,³⁹ A. Lath,⁵² G. Latino,⁴⁶ I. Lazzizzera,⁴³ T. LeCompte,² J. Lee,⁴⁹ J. Lee,²⁷ Y.J. Lee,²⁷ S.W. Lee,⁵³ R. Lefèvre,³ N. Leonardo,³² S. Leone,⁴⁶ S. Levy,¹³ J.D. Lewis,¹⁶ C. Lin,⁶⁰ C.S. Lin,¹⁶ M. Lindgren,¹⁶ E. Lipeles,⁹ A. Lister,¹⁹ D.O. Litvintsev,¹⁶ T. Liu,¹⁶ N.S. Lockyer,⁴⁵ A. Loginov,³⁶ M. Loretì,⁴³ P. Loverre,⁵¹ R.-S. Lu,¹ D. Lucchesi,⁴³ P. Lujan,²⁸ P. Lukens,¹⁶ G. Lungu,¹⁷ L. Lyons,⁴² J. Lys,²⁸ R. Lysak,¹ E. Lytken,⁴⁸ P. Mack,²⁵ D. MacQueen,³³ R. Madrak,¹⁶ K. Maeshima,¹⁶ T. Maki,²² P. Maksimovic,²⁴ S. Malde,⁴² G. Manca,²⁹ F. Margaroli,⁵ R. Marginean,¹⁶ C. Marino,²³ A. Martin,⁶⁰ V. Martin,³⁸ M. Martínez,³ T. Maruyama,⁵⁵ P. Mastrandrea,⁵¹ H. Matsunaga,⁵⁵ M.E. Mattson,⁵⁸ R. Mazini,³³ P. Mazzanti,⁵ K.S. McFarland,⁴⁹ P. McIntyre,⁵³ R. McNulty,²⁹ A. Mehta,²⁹ S. Menzemer,¹¹ A. Menzione,⁴⁶ P. Merkel,⁴⁸ C. Mesropian,⁵⁰ A. Messina,⁵¹ M. von der Mey,⁸ T. Miao,¹⁶ N. Miladinovic,⁶ J. Miles,³² R. Miller,³⁵ J.S. Miller,³⁴ C. Mills,¹⁰ M. Milnik,²⁵ R. Miquel,²⁸ A. Mitra,¹ G. Mitselmakher,¹⁷ A. Miyamoto,²⁶ N. Moggi,⁵ B. Mohr,⁸ R. Moore,¹⁶

M. Morello,⁴⁶ P. Movilla Fernandez,²⁸ J. Mülmenstädt,²⁸ A. Mukherjee,¹⁶ Th. Muller,²⁵ R. Mumford,²⁴ P. Murat,¹⁶ J. Nachtman,¹⁶ J. Naganoma,⁵⁷ S. Nahn,³² I. Nakano,⁴⁰ A. Napier,⁵⁶ D. Naumov,³⁷ V. Necula,¹⁷ C. Neu,⁴⁵ M.S. Neubauer,⁹ J. Nielsen,²⁸ T. Nigmanov,⁴⁷ L. Nodulman,² O. Norniella,³ E. Nurse,³⁰ T. Ogawa,⁵⁷ S.H. Oh,¹⁵ Y.D. Oh,²⁷ T. Okusawa,⁴¹ R. Oldeman,²⁹ R. Orava,²² K. Osterberg,²² C. Pagliarone,⁴⁶ E. Palencia,¹¹ R. Paoletti,⁴⁶ V. Papadimitriou,¹⁶ A.A. Paramonov,¹³ B. Parks,³⁹ S. Pashapour,³³ J. Patrick,¹⁶ G. Pauletta,⁵⁴ M. Paulini,¹² C. Paus,³² D.E. Pellett,⁷ A. Penzo,⁵⁴ T.J. Phillips,¹⁵ G. Piacentino,⁴⁶ J. Piedra,⁴⁴ L. Pinera,¹⁷ K. Pitts,²³ C. Plager,⁸ L. Pondrom,⁵⁹ X. Portell,³ O. Poukhov,¹⁴ N. Pounder,⁴² F. Prakoshyn,¹⁴ A. Pronko,¹⁶ J. Proudfoot,² F. Ptohos,¹⁸ G. Punzi,⁴⁶ J. Pursley,²⁴ J. Rademacker,⁴² A. Rahaman,⁴⁷ A. Rakitin,³² S. Rappoccio,²¹ F. Ratnikov,⁵² B. Reisert,¹⁶ V. Rekovic,³⁷ N. van Remortel,²² P. Renton,⁴² M. Rescigno,⁵¹ S. Richter,²⁵ F. Rimondi,⁵ L. Ristori,⁴⁶ W.J. Robertson,¹⁵ A. Robson,²⁰ T. Rodrigo,¹¹ E. Rogers,²³ S. Rolli,⁵⁶ R. Roser,¹⁶ M. Rossi,⁵⁴ R. Rossin,¹⁷ C. Rott,⁴⁸ A. Ruiz,¹¹ J. Russ,¹² V. Rusu,¹³ H. Saarikko,²² S. Sabik,³³ A. Safonov,⁵³ W.K. Sakumoto,⁴⁹ G. Salamanna,⁵¹ O. Saltó,³ D. Saltzberg,⁸ C. Sanchez,³ L. Santi,⁵⁴ S. Sarkar,⁵¹ L. Sartori,⁴⁶ K. Sato,⁵⁵ P. Savard,³³ A. Savoy-Navarro,⁴⁴ T. Scheidle,²⁵ P. Schlabach,¹⁶ E.E. Schmidt,¹⁶ M.P. Schmidt,⁶⁰ M. Schmitt,³⁸ T. Schwarz,³⁴ L. Scodellaro,¹¹ A.L. Scott,¹⁰ A. Scribano,⁴⁶ F. Scuri,⁴⁶ A. Sedov,⁴⁸ S. Seidel,³⁷ Y. Seiya,⁴¹ A. Semenov,¹⁴ L. Sexton-Kennedy,¹⁶ I. Sfiligoi,¹⁸ M.D. Shapiro,²⁸ T. Shears,²⁹ P.F. Shepard,⁴⁷ D. Sherman,²¹ M. Shimojima,⁵⁵ M. Shochet,¹³ Y. Shon,⁵⁹ I. Shreyber,³⁶ A. Sidoti,⁴⁴ P. Sinervo,³³ A. Sisakyan,¹⁴ J. Sjolín,⁴² A. Skiba,²⁵ A.J. Slaughter,¹⁶ K. Sliwa,⁵⁶ J.R. Smith,⁷ F.D. Snider,¹⁶ R. Snihur,³³ M. Soderberg,³⁴ A. Soha,⁷ S. Somalwar,⁵² V. Sorin,³⁵ J. Spalding,¹⁶ M. Spezziga,¹⁶ F. Spinella,⁴⁶ T. Spreitzer,³³ P. Squillacioti,⁴⁶ M. Stanitzki,⁶⁰ A. Staveris-Polykalas,⁴⁶ R. St. Denis,²⁰ B. Stelzer,⁸ O. Stelzer-Chilton,⁴² D. Stentz,³⁸ J. Strologas,³⁷ D. Stuart,¹⁰ J.S. Suh,²⁷ A. Sukhanov,¹⁷ K. Sumorok,³² H. Sun,⁵⁶ T. Suzuki,⁵⁵ A. Taffard,²³ R. Takashima,⁴⁰ Y. Takeuchi,⁵⁵ K. Takikawa,⁵⁵ M. Tanaka,² R. Tanaka,⁴⁰ N. Tanimoto,⁴⁰ M. Tecchio,³⁴ P.K. Teng,¹ K. Terashi,⁵⁰ S. Tether,³² J. Thom,¹⁶ A.S. Thompson,²⁰ E. Thomson,⁴⁵ P. Tipton,⁴⁹ V. Tiwari,¹² S. Tkaczyk,¹⁶ D. Toback,⁵³ S. Tokar,¹⁴ K. Tollefson,³⁵ T. Tomura,⁵⁵ D. Tonelli,⁴⁶ M. Tönnemann,³⁵ S. Torre,¹⁸ D. Torretta,¹⁶ S. Tourneur,⁴⁴ W. Trischuk,³³ R. Tsuchiya,⁵⁷ S. Tsuno,⁴⁰ N. Turini,⁴⁶ F. Ukegawa,⁵⁵ T. Unverhau,²⁰ S. Uozumi,⁵⁵ D. Usynin,⁴⁵ A. Vaiciulis,⁴⁹ S. Vallecorsa,¹⁹ A. Varganov,³⁴ E. Vataga,³⁷ G. Velev,¹⁶ G. Veramendi,²³ V. Veszpremi,⁴⁸ R. Vidal,¹⁶ I. Vila,¹¹ R. Vilar,¹¹ T. Vine,³⁰ I. Vollrath,³³ I. Volobouev,²⁸ G. Volpi,⁴⁶ F. Würthwein,⁹ P. Wagner,⁵³ R. G. Wagner,² R.L. Wagner,¹⁶ W. Wagner,²⁵ R. Wallny,⁸ T. Walter,²⁵ Z. Wan,⁵² S.M. Wang,¹ A. Warburton,³³ S. Waschke,²⁰ D. Waters,³⁰ W.C. Wester III,¹⁶ B. Whitehouse,⁵⁶ D. Whiteson,⁴⁵ A.B. Wicklund,² E. Wicklund,¹⁶ G. Williams,³³ H.H. Williams,⁴⁵ P. Wilson,¹⁶ B.L. Winer,³⁹ P. Wittich,¹⁶ S. Wolbers,¹⁶ C. Wolfe,¹³ T. Wright,³⁴ X. Wu,¹⁹ S.M. Wynne,²⁹ A. Yagil,¹⁶ K. Yamamoto,⁴¹ J. Yamaoka,⁵² T. Yamashita,⁴⁰ C. Yang,⁶⁰ U.K. Yang,¹³ Y.C. Yang,²⁷ W.M. Yao,²⁸ G.P. Yeh,¹⁶ J. Yoh,¹⁶ K. Yorita,¹³ T. Yoshida,⁴¹ G.B. Yu,⁴⁹ I. Yu,²⁷ S.S. Yu,¹⁶ J.C. Yun,¹⁶ L. Zanello,⁵¹ A. Zanetti,⁵⁴ I. Zaw,²¹ F. Zetti,⁴⁶ X. Zhang,²³ J. Zhou,⁵² and S. Zucchelli⁵

(CDF Collaboration)

¹*Institute of Physics, Academia Sinica, Taipei, Taiwan 11529, Republic of China*

²*Argonne National Laboratory, Argonne, Illinois 60439*

³*Institut de Física d'Altes Energies, Universitat Autònoma de Barcelona, E-08193, Bellaterra (Barcelona), Spain*

⁴*Baylor University, Waco, Texas 76798*

⁵*Istituto Nazionale di Fisica Nucleare, University of Bologna, I-40127 Bologna, Italy*

⁶*Brandeis University, Waltham, Massachusetts 02254*

⁷*University of California, Davis, Davis, California 95616*

⁸*University of California, Los Angeles, Los Angeles, California 90024*

⁹*University of California, San Diego, La Jolla, California 92093*

¹⁰*University of California, Santa Barbara, Santa Barbara, California 93106*

¹¹*Instituto de Física de Cantabria, CSIC-University of Cantabria, 39005 Santander, Spain*

¹²*Carnegie Mellon University, Pittsburgh, PA 15213*

¹³*Enrico Fermi Institute, University of Chicago, Chicago, Illinois 60637*

¹⁴*Joint Institute for Nuclear Research, RU-141980 Dubna, Russia*

¹⁵*Duke University, Durham, North Carolina 27708*

¹⁶*Fermi National Accelerator Laboratory, Batavia, Illinois 60510*

¹⁷*University of Florida, Gainesville, Florida 32611*

¹⁸*Laboratori Nazionali di Frascati, Istituto Nazionale di Fisica Nucleare, I-00044 Frascati, Italy*

¹⁹*University of Geneva, CH-1211 Geneva 4, Switzerland*

²⁰*Glasgow University, Glasgow G12 8QQ, United Kingdom*

²¹*Harvard University, Cambridge, Massachusetts 02138*

- ²²*Division of High Energy Physics, Department of Physics,
University of Helsinki and Helsinki Institute of Physics, FIN-00014, Helsinki, Finland*
- ²³*University of Illinois, Urbana, Illinois 61801*
- ²⁴*The Johns Hopkins University, Baltimore, Maryland 21218*
- ²⁵*Institut für Experimentelle Kernphysik, Universität Karlsruhe, 76128 Karlsruhe, Germany*
- ²⁶*High Energy Accelerator Research Organization (KEK), Tsukuba, Ibaraki 305, Japan*
- ²⁷*Center for High Energy Physics: Kyungpook National University,
Taegu 702-701, Korea; Seoul National University, Seoul 151-742,
Korea; and SungKyunKwan University, Suwon 440-746, Korea*
- ²⁸*Ernest Orlando Lawrence Berkeley National Laboratory, Berkeley, California 94720*
- ²⁹*University of Liverpool, Liverpool L69 7ZE, United Kingdom*
- ³⁰*University College London, London WC1E 6BT, United Kingdom*
- ³¹*Centro de Investigaciones Energeticas Medioambientales y Tecnologicas, E-28040 Madrid, Spain*
- ³²*Massachusetts Institute of Technology, Cambridge, Massachusetts 02139*
- ³³*Institute of Particle Physics: McGill University, Montréal,
Canada H3A 2T8; and University of Toronto, Toronto, Canada M5S 1A7*
- ³⁴*University of Michigan, Ann Arbor, Michigan 48109*
- ³⁵*Michigan State University, East Lansing, Michigan 48824*
- ³⁶*Institution for Theoretical and Experimental Physics, ITEP, Moscow 117259, Russia*
- ³⁷*University of New Mexico, Albuquerque, New Mexico 87131*
- ³⁸*Northwestern University, Evanston, Illinois 60208*
- ³⁹*The Ohio State University, Columbus, Ohio 43210*
- ⁴⁰*Okayama University, Okayama 700-8530, Japan*
- ⁴¹*Osaka City University, Osaka 588, Japan*
- ⁴²*University of Oxford, Oxford OX1 3RH, United Kingdom*
- ⁴³*University of Padova, Istituto Nazionale di Fisica Nucleare,
Sezione di Padova-Trento, I-35131 Padova, Italy*
- ⁴⁴*LPNHE, Universite Pierre et Marie Curie/IN2P3-CNRS, UMR7585, Paris, F-75252 France*
- ⁴⁵*University of Pennsylvania, Philadelphia, Pennsylvania 19104*
- ⁴⁶*Istituto Nazionale di Fisica Nucleare Pisa, Universities of Pisa,
Siena and Scuola Normale Superiore, I-56127 Pisa, Italy*
- ⁴⁷*University of Pittsburgh, Pittsburgh, Pennsylvania 15260*
- ⁴⁸*Purdue University, West Lafayette, Indiana 47907*
- ⁴⁹*University of Rochester, Rochester, New York 14627*
- ⁵⁰*The Rockefeller University, New York, New York 10021*
- ⁵¹*Istituto Nazionale di Fisica Nucleare, Sezione di Roma 1,
University of Rome “La Sapienza,” I-00185 Roma, Italy*
- ⁵²*Rutgers University, Piscataway, New Jersey 08855*
- ⁵³*Texas A&M University, College Station, Texas 77843*
- ⁵⁴*Istituto Nazionale di Fisica Nucleare, University of Trieste/ Udine, Italy*
- ⁵⁵*University of Tsukuba, Tsukuba, Ibaraki 305, Japan*
- ⁵⁶*Tufts University, Medford, Massachusetts 02155*
- ⁵⁷*Waseda University, Tokyo 169, Japan*
- ⁵⁸*Wayne State University, Detroit, Michigan 48201*
- ⁵⁹*University of Wisconsin, Madison, Wisconsin 53706*
- ⁶⁰*Yale University, New Haven, Connecticut 06520*

(Dated: February 6, 2018)

We search for decays of the type $B_{(s)}^0 \rightarrow h^+h'^-$ (where $h, h' = K$ or π) in 180 pb^{-1} of $\bar{p}p$ collisions collected at the Tevatron by the upgraded Collider Detector at Fermilab. We report the first observation of the new mode $B_s^0 \rightarrow K^+K^-$ with a yield of 236 ± 32 events, corresponding to $(f_s/f_d) \times \mathcal{B}(B_s^0 \rightarrow K^+K^-)/\mathcal{B}(B^0 \rightarrow K^+\pi^-) = 0.46 \pm 0.08(\text{stat.}) \pm 0.07(\text{syst.})$, where f_s/f_d is the ratio of production fractions of B_s^0 and B^0 . We find results in agreement with world averages for the B^0 modes, and set the following new limits at 90% CL: $\mathcal{B}(B_s^0 \rightarrow K^-\pi^+) < 5.6 \times 10^{-6}$ and $\mathcal{B}(B_s^0 \rightarrow \pi^+\pi^-) < 1.7 \times 10^{-6}$.

PACS numbers: 13.25.Hw 14.40.Nd

The decay modes of B mesons into pairs of charmless pseudoscalar mesons are effective probes of the quark-mixing (Cabibbo-Kobayashi-Maskawa, CKM) matrix and are sensitive to potential new physics effects. Their branching fractions and CP asymmetries can be

predicted with good accuracy and compared to rich experimental data available for B^+ and B^0 mesons, produced in large quantities in $\Upsilon(4S)$ decays [1]. Measurements of similar modes predicted, but not yet observed, for the B_s^0 meson are important to complete our under-

standing of B meson decays. The measurement of observables from both strange and non-strange B mesons allows a cancellation of hadronic uncertainties, thus enhancing the precision of the extraction of physics parameters from experimental data [2, 3, 4, 5].

The branching fraction of the $B_s^0 \rightarrow K^+K^-$ mode is a candidate for observing an unusually large breaking of U-spin symmetry, and is sensitive to anomalous electroweak penguin contributions from new physics [4, 6, 7]. A combination of $B^0 \rightarrow \pi^+\pi^-$ and $B_s^0 \rightarrow K^+K^-$ observables has been proposed as a way to directly determine the phase of the V_{ub} element of the CKM matrix (angle γ), or alternatively as a test of our understanding of dynamics of B hadron decays, when compared with other determinations of γ [8]. The $B_s^0 \rightarrow K^-\pi^+$ mode can also be used in measuring γ [3], and its CP asymmetry is a powerful model-independent test [9] of the source of the direct CP asymmetry observed in the $B^0 \rightarrow K^+\pi^-$ mode [10]. The $B_s^0 \rightarrow \pi^+\pi^-$ mode proceeds only through annihilation diagrams, which are currently poorly known and a source of significant uncertainty in many theoretical calculations [11]. Its features are similar to the as yet unobserved $B^0 \rightarrow K^+K^-$ mode, but it has a larger predicted branching fraction [11, 12]; a measurement of both modes would allow a determination of the strength of penguin-annihilation [4].

In this letter we report the first observation of the decay $B_s^0 \rightarrow K^+K^-$ and perform the first measurement in hadron collisions of partial widths of $B_{(s)}^0$ decays to pairs of charged pions and kaons. Throughout this paper, C-conjugate modes are implied and branching fractions indicate CP-averages unless otherwise stated.

The measurements have been performed in a sample of 180 pb^{-1} of $\bar{p}p$ collisions at $\sqrt{s} = 1.96 \text{ TeV}$, recorded at the Tevatron collider by the upgraded Collider Detector at Fermilab (CDF II). CDF II is a multipurpose magnetic spectrometer surrounded by calorimeters and muon detectors [13]. The components of the detector pertinent to this analysis are described briefly below. A silicon microstrip detector (SVX II) [14] and a cylindrical drift chamber (COT) [15] immersed in a 1.4 T solenoidal magnetic field allow reconstruction of charged particles in the pseudorapidity range $|\eta| < 1.0$ [16]. The SVX II consists of five concentric layers of double-sided silicon detectors with radii between 2.5 and 10.6 cm, each providing a measurement with $15 \mu\text{m}$ resolution in the ϕ direction. The COT has 96 measurement layers, between 40 and 137 cm in radius, organized into alternating axial and $\pm 2^\circ$ stereo superlayers. The transverse momentum resolution is $\sigma_{p_T}/p_T \simeq 0.15\% p_T/(\text{GeV}/c)$. The specific energy loss (dE/dx) of charged particles in the COT can be measured from the collected charge, which is encoded in the output pulse-width of each wire.

Data were collected by a three-level trigger system, using a set of requirements dedicated to B hadron decays into charged particle pairs. At Level 1, charged particle

tracks are reconstructed in the COT transverse plane by a hardware processor (XFT) [17]. Two opposite-curvature tracks are required, with reconstructed transverse momenta $p_{T1}, p_{T2} > 2 \text{ GeV}/c$, the scalar sum $p_{T1} + p_{T2} > 5.5 \text{ GeV}/c$, and a transverse opening-angle $\Delta\phi < 135^\circ$. At Level 2, the Silicon Vertex Trigger (SVT) [18] combines XFT tracks with SVX II hits to measure the impact parameter d (distance of closest approach to the beam line) of each valid track. The requirement of two tracks with $100 \mu\text{m} < d < 1.0 \text{ mm}$ reduces light-quark background by two orders of magnitude while preserving $\simeq 50\%$ of the signal. A tighter opening angle cut: $20^\circ < \Delta\phi < 135^\circ$ selects two-body B decays from multi-body with 97% efficiency and reduces background further. Each track pair is then used to form a B candidate, which is required to have an impact parameter relative to the beam axis $d_B < 140 \mu\text{m}$ and to have travelled a transverse distance $L_{xy} > 200 \mu\text{m}$. At Level 3, a farm of computers confirms the selection with a full event reconstruction. The overall acceptance of the trigger selection is $\simeq 2\%$ for B mesons of $p_T > 4 \text{ GeV}/c$.

In the offline analysis, combinatoric and light-quark backgrounds are effectively rejected by requiring the B candidate to be isolated. The isolation cut ($I > 0.5$) [19] has been chosen, together with tightened cuts on kinematic observables ($L_{xy} > 300 \mu\text{m}$, $d_B < 80 \mu\text{m}$, and $d > 150 \mu\text{m}$), by maximizing the quantity $S/(S+B)^{1/2}$ over all possible combinations of cuts. The background B is estimated from the data sidebands. The expected signal yield S is obtained from a detailed detector simulation assuming the momentum distribution of B -mesons measured by CDF [20], and normalized to the yield observed after the trigger selection. The overall efficiency of the chosen offline selection is $\simeq 50\%$.

No more than one B meson candidate per event survives the selection, and a mass is assigned to each, assuming the pion mass for both decay products. The mass distribution, shown in Fig. 1, exhibits an obvious peak in the $B_{(s)}^0$ mass region. A binned fit of a Gaussian over an exponential background provides an estimate of 893 ± 47 signal events, with a width $\sigma = 38 \pm 2 \text{ MeV}/c^2$, compared to an expected mass resolution $\sigma = 28 \text{ MeV}/c^2$ for an individual $B_{(s)}^0 \rightarrow h^+h'^-$ mode. This indicates the presence of at least two distinct final states. Sizable signal contributions are expected from two known B^0 modes, $B^0 \rightarrow \pi^+\pi^-$ and $B^0 \rightarrow K^+\pi^-$, and two as yet unobserved B_s^0 modes, $B_s^0 \rightarrow K^+K^-$ and $B_s^0 \rightarrow K^-\pi^+$. Figure 1 shows that, as expected, the different modes are too closely spaced in mass to be clearly resolved and appear instead as a single peak somewhat broader than the mass resolution. In addition to mass resolution, we use kinematic information along with particle identification to extract the different contribution. We incorporate all information in an unbinned likelihood fit, to statistically determine the contribution of each mode, and the CP asymmetry of the $B^0 \rightarrow K^+\pi^-$ mode

$$A_{CP} = [N(\bar{B}) - N(B)]/[N(\bar{B}) + N(B)].$$

For the kinematic portion, we use two loosely correlated observables to summarize the information carried by all possible values of invariant mass of the candidate B , resulting from different mass assignments to the two outgoing particles [21]. They are the mass $M_{\pi\pi}$ calculated with the pion mass assignment to both particles, and the signed momentum imbalance $\alpha = (1 - p_1/p_2)q_1$, where p_1 (p_2) is the lower (higher) of the particle momenta, and q_1 is the sign of the charge of the particle of momentum p_1 . Using these two variables, the mass of any particular mode can be expressed, in the relativistic limit, as:

$$M_{m_1 m_2}^2 = M_{\pi\pi}^2 - (2 - |\alpha|)(m_2^2 - m_\pi^2) - [1 - (|\alpha| - 1)^{-1}](m_1^2 - m_\pi^2) \quad (1)$$

where m_1 (m_2) is the mass of the lower (higher) momentum particle (Fig. 2, left). Particle identification (PID)

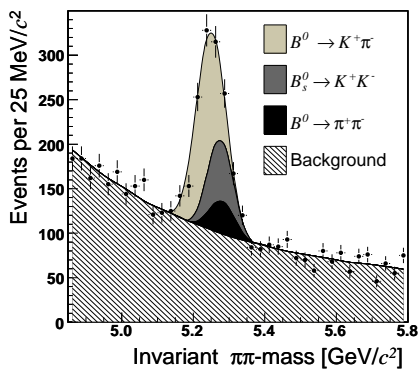


FIG. 1: Invariant mass distribution of $B_{(s)}^0 \rightarrow h^+ h'^-$ candidates passing all selection requirements, using a pion mass assumption for both decay products. Cumulative projections of the likelihood fit for each mode are overlaid.

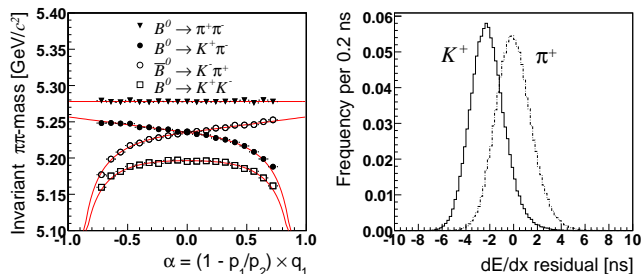


FIG. 2: (left) Average $M_{\pi\pi}$ versus α for simulated samples of B^0 events, where $K^+ \pi^-$ and $K^- \pi^+$ are treated separately. The solid curves are the corresponding first-order expressions from Eq. (1). The corresponding plots for the B_s^0 are similar, but shifted for the mass difference. (right) Distribution of dE/dx (mean COT pulse-width) around the average pion response, for calibration samples of kaons and pions (see text).

information is provided by the measured dE/dx of the two tracks. In order to account for their dependence on particle momentum, we include in our fit the scalar sum $p_{\text{tot}} = p_1 + p_2$ as a fifth observable, which in conjunction with α provides unique identification of the momenta of both particles.

With the chosen observables, the likelihood contribution of the i^{th} event is written as:

$$\mathcal{L}_i = (1 - b) \sum_j f_j \mathcal{L}_j^{\text{kin}} \mathcal{L}_j^{\text{PID}} + b \mathcal{L}_{\text{bck}}^{\text{kin}} \mathcal{L}_{\text{bck}}^{\text{PID}} \quad (2)$$

where the index ‘bck’ labels background-related quantities, the index j runs over the eight distinguishable $B_{(s)}^0 \rightarrow h^+ h'^-$ modes (Fig. 2), and f_j are their fractions, to be determined by the fit together with the background fraction b . The $\mathcal{L}_j^{\text{kin}}$ is given by the product of the conditional probability density of $M_{\pi\pi}$ for given α and the joint probability distribution $P_j(\alpha, p_{\text{tot}})$. The mass distribution is a Gaussian centered at the value of $M_{\pi\pi}$ obtained from Eq. (1) by setting the appropriate particle masses for each decay mode j . The Gaussian width $\sigma_M = 28 \pm 3$ MeV/ c^2 was interpolated from the observed widths of other two-body decays ($D^0 \rightarrow K^- \pi^+$, $J/\psi \rightarrow \mu^+ \mu^-$, and $\Upsilon \rightarrow \mu^+ \mu^-$), and the B^0 and B_s^0 masses are set to the values measured by CDF [22] to cancel the common systematic uncertainty. The background mass distribution is fitted to an exponential function plus a constant. The $P_j(\alpha, p_{\text{tot}})$ is parameterized for each mode j by a product of polynomial and exponential functions, fitted to Monte Carlo samples produced by a detailed detector simulation, while the corresponding distribution for the background is obtained from the mass sidebands of data.

The dE/dx response was calibrated over the tracking volume and time by means of a 97%-pure sample of $3 \times 10^5 D^{*+} \rightarrow D^0 \pi^+ \rightarrow [K^- \pi^+] \pi^+$ decays, where the D^0 decay products are identified by the charge of the D^{*+} pion [23]. The observed response (Fig. 2, right) is well-modeled by the convolution of a single-particle response function with a common baseline fluctuation, causing a 10% correlation between particles in the same event. Both effects are quasi-Gaussian with small tails, and have been accurately modeled in \mathcal{L}^{PID} . The separation between pions and kaons in the range $2 < p_T < 10$ GeV/ c is nearly constant at 1.4 standard deviations, corresponding to a resolution 1.7 times worse than a ‘‘perfect’’ PID, when measuring the relative fractions of the two particles in any given sample. The $\mathcal{L}_{\text{bck}}^{\text{PID}}$ term allows for independent pion, kaon, proton, and electron components, which are free to vary independently in three mass regions (left, under, and right of the signal peak) to allow for possible variations due to the contribution of partially-reconstructed B hadrons in the lower-mass region. Muons are indistinguishable from pions with the available dE/dx resolution.

The fit of the data sample returns the yields listed in Table I. The observed resolutions are compatible with ex-

pectations from fitting Monte Carlo samples of the same size. Significant signals are seen for $B^0 \rightarrow \pi^+\pi^-$, $B^0 \rightarrow K^+\pi^-$, and the previously unobserved $B_s^0 \rightarrow K^+K^-$ mode, while no evidence is obtained for $B_s^0 \rightarrow K^-\pi^+$, $B_s^0 \rightarrow \pi^+\pi^-$, or $B^0 \rightarrow K^+K^-$. As a check of our results, we performed an alternative fit based solely on kinematical information. Since the $B^0 \rightarrow \pi^+\pi^-$ mode is indistinguishable from $B_s^0 \rightarrow K^+K^-$ in absence of PID information, we constrain its rate to its world-average value [24]. This fit confirms the main results, returning a yield of $193 \pm 55 B_s^0 \rightarrow K^+K^-$ events. To convert raw yields into relative branching fractions, we apply corrections for the different efficiencies of trigger and offline selection requirements for different decay modes; the relative efficiency corrections between modes do not exceed 19%. Most corrections are determined from the detailed detector simulation, with the following exceptions which are measured using data: A momentum-averaged relative isolation efficiency between B_s^0 and B^0 of 1.07 ± 0.11 has been determined from fully-reconstructed samples of $B_s^0 \rightarrow J/\psi \phi$, $B_s^0 \rightarrow D_s^- \pi^+$, $B^0 \rightarrow J/\psi K^{*0}$, and $B^0 \rightarrow D^- \pi^+$. The lower specific ionization of kaons with respect to pions in the COT is responsible for a $\simeq 5\%$ lower efficiency to reconstruct a kaon by the XFT. This effect is measured in a sample of $D^+ \rightarrow K^- \pi^+ \pi^+$ decays triggered on two tracks, using the unbiased third track. The only correction needed by A_{CP} is a $(1.0 \pm 0.25)\%$ shift due to the different probability for K^+ and K^- to interact with the tracker material. The accuracy of our control over instrumental charge asymmetries is confirmed by the smallness of the asymmetry ($< 0.5\%$) measured in the $D^0 \rightarrow K^- \pi^+$ mode [25]. The $B_s^0 \rightarrow K^+K^-$ and $B_s^0 \rightarrow \pi^+\pi^-$ modes require a special treatment, since they contain a superposition of the flavor eigenstates of the B_s^0 . Their time evolution might differ from the flavor-specific modes if the width difference $\Delta\Gamma_s$ between the B_s^0 mass eigenstates is significant. The current result is derived under the assumption that both modes are dominated by the short-lived B_s^0 component, that $\Gamma_s = \Gamma_d$, and $\Delta\Gamma_s/\Gamma_s = 0.12 \pm 0.06$ [26]. The latter uncertainty is included in estimating the overall systematic uncertainty.

The dominant contributions to the systematic uncertainty are: the statistical uncertainty on isolation efficiency (B_s^0 modes), possible charge asymmetry of background (A_{CP}), and final state photon radiation ($B^0 \rightarrow \pi^+\pi^-$). The latter is conservatively estimated with the full effect predicted by QED calculations [27]. Smaller systematic uncertainties are assigned for: mass scale and resolution; dE/dx response model; trigger efficiencies; background shape and kinematics; B meson masses, lifetimes, and differences in momenta, allowed to vary by a factor $(m_{B_s^0} - m_{B^0})/m_{B^0}$ due to fragmentation effects [28].

The relative branching fractions obtained after applying all corrections are listed in Table I, where f_d and f_s indicate the production fractions respectively of B^0

and B_s^0 from fragmentation of a b quark in $\bar{p}p$ collisions. Upper limits are quoted for modes in which no significant signal is observed [29]. We also list absolute results obtained by normalizing our data to the world-average of $\mathcal{B}(B^0 \rightarrow K^+\pi^-)$ and assuming for f_s/f_d the world-average from $\bar{p}p$ and e^+e^- experiments [24].

The rate of the newly observed mode $B_s^0 \rightarrow K^+K^-$ favors the higher value $(36 \pm 7) \times 10^{-6}$ predicted by calculations based on QCD sum rules [4, 6] implying large U-spin breaking in this process, although it is not statistically incompatible with the expectation $\mathcal{B}(B_s^0 \rightarrow K^+K^-) = \mathcal{B}(B^0 \rightarrow K^+\pi^-)$ from the assumption of exact U-spin symmetry and negligible spectator contributions. We also derive the ratio of U-spin-conjugate decays: $(f_d/f_s) \times \mathcal{B}(B^0 \rightarrow \pi^+\pi^-)/\mathcal{B}(B_s^0 \rightarrow K^+K^-) = 0.45 \pm 0.13 \pm 0.06$, which can be related to the CP asymmetries in the $B^0 \rightarrow \pi^+\pi^-$ mode and to the CKM angle γ [8]. Our results for the B^0 are in agreement with world average values: $\mathcal{B}(B^0 \rightarrow \pi^+\pi^-) = (4.6 \pm 0.4) \times 10^{-6}$ and $A_{CP}(B^0 \rightarrow K^+\pi^-) = -0.113 \pm 0.020$ [30] although our A_{CP} measurement is also compatible with zero. The limit set on $B_s^0 \rightarrow K^- \pi^+$ indicates a value at the lower end of current expectations [5, 11]. The limit for the annihilation mode $B_s^0 \rightarrow \pi^+\pi^-$ is a large improvement over the previous best limit [31], approaching the expectations from recent calculations [12, 32].

In summary, we have measured relative branching fractions of $B_{(s)}^0$ mesons into pairs of charmless charged mesons. We find results in agreement with current world averages for B^0 modes and observe for the first time the $B_s^0 \rightarrow K^+K^-$ mode. We set upper limits on unobserved modes $B^0 \rightarrow K^+K^-$, $B_s^0 \rightarrow K^- \pi^+$, and $B_s^0 \rightarrow \pi^+\pi^-$.

We thank the Fermilab staff and the technical staffs of the participating institutions for their vital contributions. This work was supported by the U.S. Department of Energy and National Science Foundation; the Italian Istituto Nazionale di Fisica Nucleare; the Ministry of Education, Culture, Sports, Science and Technology of Japan; the Natural Sciences and Engineering Research Council of Canada; the National Science Council of the Republic of China; the Swiss National Science Foundation; the A.P. Sloan Foundation; the Bundesministerium für Bildung und Forschung, Germany; the Korean Science and Engineering Foundation and the Korean Research Foundation; the Particle Physics and Astronomy Research Council and the Royal Society, UK; the Russian Foundation for Basic Research; the Comisión Interministerial de Ciencia y Tecnología, Spain; the European Community's Human Potential Programme under contract HPRN-CT-2002-00292; and the Academy of Finland.

TABLE I: Summary of results. The yields of the two annihilation modes (last two rows) were fixed to zero when fitting for the four main modes. Absolute branching fractions are normalized to the the world-average values $\mathcal{B}(B^0 \rightarrow K^+\pi^-) = (18.9 \pm 0.7) \times 10^{-6}$ and $f_s/f_d = 0.26 \pm 0.039$ [24]. The first quoted uncertainty is statistical, the second is systematic.

Mode	Yield	Measured Quantity	Derived \mathcal{B} (10^{-6})
$B^0 \rightarrow K^+\pi^-$	542 ± 30	$A_{\text{CP}} = -0.013 \pm 0.078 \pm 0.012$	
$B^0 \rightarrow \pi^+\pi^-$	121 ± 27	$\frac{\mathcal{B}(B^0 \rightarrow \pi^+\pi^-)}{\mathcal{B}(B^0 \rightarrow K^+\pi^-)} = 0.21 \pm 0.05 \pm 0.03$	$3.9 \pm 1.0 \pm 0.6$
$B_s^0 \rightarrow K^+K^-$	236 ± 32	$\frac{f_s}{f_d} \frac{\mathcal{B}(B_s^0 \rightarrow K^+K^-)}{\mathcal{B}(B^0 \rightarrow K^+\pi^-)} = 0.46 \pm 0.08 \pm 0.07$	$33 \pm 6 \pm 7$
$B_s^0 \rightarrow K^-\pi^+$	3 ± 25	$\frac{f_s}{f_d} \frac{\mathcal{B}(B_s^0 \rightarrow K^-\pi^+)}{\mathcal{B}(B^0 \rightarrow K^+\pi^-)} < 0.08$ @ 90% CL	< 5.6 @ 90% CL
$B_s^0 \rightarrow \pi^+\pi^-$	-10 ± 15	$\frac{\mathcal{B}(B_s^0 \rightarrow \pi^+\pi^-)}{\mathcal{B}(B^0 \rightarrow K^+K^-)} < 0.05$ @ 90% CL	< 1.7 @ 90% CL
$B^0 \rightarrow K^+K^-$	10 ± 23	$\frac{\mathcal{B}(B^0 \rightarrow K^+K^-)}{\mathcal{B}(B^0 \rightarrow K^+\pi^-)} < 0.10$ @ 90% CL	< 1.8 @ 90% CL

- [1] B. Aubert *et al.* (BaBar Collaboration), Phys. Rev. Lett. **89**, 281802 (2002); Y. Chao *et al.* (Belle Collaboration), Phys. Rev. D **69**, 111102 (2004); A. Bornheim *et al.* (CLEO Collaboration), Phys. Rev. D **68**, 052002 (2003); B. Aubert *et al.* (BaBar Collaboration), arXiv:hep-ex/0508046.
- [2] M. Gronau, Phys. Lett. B **492**, 297 (2000).
- [3] M. Gronau and J. L. Rosner, Phys. Lett. B **482**, 71 (2000).
- [4] A. J. Buras *et al.*, Nucl. Phys. B **697**, 133 (2004).
- [5] J. F. Sun, G. H. Zhu, and D. S. Du, Phys. Rev. D **68**, 054003 (2003).
- [6] A. Khodjamirian, T. Mannel, and M. Melcher, Phys. Rev. D **68**, 114007 (2003).
- [7] S. Descotes-Genon, J. Matias and J. Virto, Phys. Rev. Lett. **97**, 061801 (2006).
- [8] R. Fleischer, Phys. Lett. B **459**, 306 (1999); D. London and J. Matias, Phys. Rev. D **70**, 031502(R) (2004).
- [9] H. J. Lipkin, Phys. Lett. B **621**, 126 (2005).
- [10] B. Aubert *et al.* (BaBar Collaboration), Phys. Rev. Lett. **93**, 131801 (2004); Y. Chao *et al.* (Belle Collaboration), Phys. Rev. Lett. **93**, 191802 (2004).
- [11] M. Beneke and M. Neubert, Nucl. Phys. B **675**, 333 (2003).
- [12] Y. D. Yang, F. Su, G. R. Lu, and H. J. Hao, Eur. Phys. J. C **44**, 243 (2005).
- [13] D. Acosta *et al.* (CDF Collaboration), Phys. Rev. D **71**, 032001 (2005).
- [14] A. Sill *et al.*, Nucl. Instrum. Methods **A 447**, 1 (2000).
- [15] T. Affolder *et al.*, Nucl. Instrum. Methods **A 526**, 249 (2004).
- [16] CDF II uses a cylindrical coordinate system in which ϕ is the azimuthal angle, r is the radius from the nominal beam line, and z points in the proton beam direction, with the origin at the center of the detector. The transverse plane is the plane perpendicular to the z axis.
- [17] E. J. Thomson *et al.*, IEEE Trans. Nucl. Sci. **49**, 1063 (2002).
- [18] W. Ashmanskas *et al.*, Nucl. Instrum. Methods, **A518**, 532 (2004).
- [19] Isolation is defined as $I = p_T(B)/(\sum_i p_{Ti})$, where $p_T(B)$ is the transverse momentum of the B candidate, and the sum runs over all other tracks within a cone of radius 1 in η - ϕ space around the B flight-direction.
- [20] D. Acosta *et al.* (CDF Collaboration), Phys. Rev. D **71**, 032001 (2005).
- [21] For a discussion of the bias in multi-component fits related to the use of multiple variables see G. Punzi, in *Proceedings of PHYSTAT2003: Statistical Problems in Particle Physics, Astrophysics, and Cosmology*, eConf **C030908**, WELT002 (2003); arXiv:physics/0401045.
- [22] D. Acosta *et al.* (CDF Collaboration), Phys. Rev. Lett. **96**, 202001 (2006).
- [23] D. Tonelli, Ph.D. Thesis, Scuola Normale Superiore, Pisa (Fermilab Report No. FERMILAB-THESIS-2006-23, 2006).
- [24] E. Barberio *et al.* [Heavy Flavor Averaging Group (HFAG)], arXiv:hep-ex/0603003.
- [25] D. Acosta *et al.* (CDF Collaboration), Phys. Rev. Lett. **94**, 122001 (2005).
- [26] M. Beneke, G. Buchalla, C. Greub, A. Lenz and U. Nierste, "Next-to-leading order QCD corrections to the lifetime difference of B/s mesons," Phys. Lett. B **459** (1999) 631 [arXiv:hep-ph/9808385].
- [27] V. Cirigliano, J. F. Donoghue, and E. Golowich, Eur. Phys. J. C **18**, 83 (2000); E. Baracchini and G. Isidori, Phys. Lett. B **633**, 309 (2006).
- [28] M. L. Mangano and M. Cacciari (private communication).
- [29] We use frequentist limits based on Gaussian distribution of fit pulls (with systematics added in quadrature), and likelihood ratio ordering; see G. J. Feldman and R. D. Cousins, Phys. Rev. D **57**, 3873 (1998).
- [30] W. M. Yao *et al.* [Particle Data Group], J. Phys. G **33**, 1 (2006).
- [31] D. Buskulic *et al.* (ALEPH Collaboration), Phys. Lett. B **384**, 471 (1996).
- [32] Y. Li *et al.*, Phys. Rev. D **70**, 034009 (2004).